

Angle-dependent irreversible magnetization of an $\text{La}_{1.87}\text{Sr}_{0.13}\text{CuO}_4$ single crystal

This article has been downloaded from IOPscience. Please scroll down to see the full text article.

1993 J. Phys.: Condens. Matter 5 1883

(<http://iopscience.iop.org/0953-8984/5/12/015>)

View [the table of contents for this issue](#), or go to the [journal homepage](#) for more

Download details:

IP Address: 171.66.16.159

The article was downloaded on 12/05/2010 at 13:06

Please note that [terms and conditions apply](#).

Angle-dependent irreversible magnetization of an $\text{La}_{1.87}\text{Sr}_{0.13}\text{CuO}_4$ single crystal

Z J Yang†, K Kishio, T Kobayashi, T Kimura and S L Yuan

Department of Industrial Chemistry, University of Tokyo, Bunkyo-ku, Tokyo 113, Japan

Received 2 September 1992, in final form 21 October 1992

Abstract. Using a vibrating-sample magnetometer, the irreversible magnetization of a disc-shaped $\text{La}_{1.87}\text{Sr}_{0.13}\text{CuO}_4$ single-crystal specimen has been investigated for various angles θ between the direction of the applied field and the superconducting (Cu–O) plane. By separating the reversible and irreversible contributions from the measured magnetization induced by the applied field, we have shown that the change in the irreversible magnetic behaviour originates basically from the layered structure of the materials, and the geometrical effect on the irreversible properties is much smaller than that due to the intrinsic material anisotropy. The experimental results show that firstly the two sets of small-angle (0 and $\pi/12$) data seem to be identical, and secondly the large-angle ($\pi/6$ or greater) data can be rescaled fairly well by empirical scaling factors, which are qualitatively consistent with the scaling theory recently introduced by Blatter *et al.* These experiments also show that the scaling properties are almost temperature independent. The physical implications of the scaling approach are discussed in terms of the present results.

1. Introduction

Since the discovery of the high- T_c superconductors (HTSCs), more and more investigations have focused on the study of the physical properties of these layered structural (highly anisotropic) materials. A crucial aspect for the wide applications of the HTSCs is the irreversible magnetic behaviour. The potential applications of the HTSCs have stimulated extensive theoretical and experimental studies on their irreversible characteristics which range from fundamental investigations to tests of their practical applications.

A feature of the HTSCs which distinguishes them from the conventional superconductors is their layered structure which shows the highly anisotropic properties. On the basis of the high anisotropy, several new theoretical approaches [1–6] have been introduced to explain the novel phenomena observed in experiments [7–12]. In particular, Blatter *et al* [5] have recently introduced a scaling approach to mapping the results of isotropic superconductors to anisotropic materials.

In a recent letter, Hellman *et al* [11] measured the induced magnetization for conventional Nb and Pb–Bi superconductors. With the selection of different geometrical shapes of the specimens, they demonstrated that the irreversible contributions of the induced magnetization could also clearly be changed by changing

† Present address: Department of Physics, Dalhousie University, Halifax, NS B3H 3J5, Canada.

the direction of the applied field for the isotropic superconductors, which is generally believed to relate only to the layered structural HTSCs. Furthermore, Hellman *et al* argued that 'the interpretations of the irreversible magnetic behavior in terms of the intrinsic material anisotropy' due to the plate geometry of the specimens used in the most of the measurements should be re-examined. In order to clarify the physical picture, it is necessary to carry out angle-dependent experiments in which the geometrical effect should be avoided. However, at the present time, high-quality large $\text{YBa}_2\text{Cu}_3\text{O}_{7-\delta}$ (Y1:2:3), Bi-based and Tl-based single crystals are not available; therefore, we can perform the angle-dependent experiments on only $(\text{La}_{1-x}\text{Sr}_x)_2\text{CuO}_4$ single crystals, for which large single crystals in both the a - b plane and the c direction have been synthesized [13].

In this paper, we report an investigation of the angle-dependent magnetization of a disc-shaped $\text{La}_{1.87}\text{Sr}_{0.13}\text{CuO}_4$ single crystal. By separating the reversible and irreversible contributions from the measured magnetizations induced by the applied fields, we have unambiguously demonstrated that the irreversible characteristics of the HTSCs are dominated by the intrinsic material anisotropy: the layered structure. Our experimental results show that the irreversible magnetization exhibits two different features as a function of the angle θ between the direction of the applied field and the superconducting (Cu-O) plane.

- (i) The two sets of small-angle data show identical M versus H_a curves.
- (ii) Empirically, the large-angle data can be rescaled fairly well into a unique (angle-independent) curve.

The empirical scaling factors have been compared with the scaling theory introduced by Blatter *et al* [5] and are qualitatively consistent with this theory.

2. Experimental details

The disc-shaped specimen was cut from a high-quality $\text{La}_{1.87}\text{Sr}_{0.13}\text{CuO}_4$ single-crystal rod grown by the travelling solvent floating-zone method. The details of the crystal growth have been published in a previous paper [13]. The electrical resistivity and DC (SQUID) magnetic susceptibility measurements show that the superconducting transition temperature is about 35 K as shown in figure 1. The R versus T curves show clearly the anisotropic feature of the specimen. ρ_c (the resistivity along the c direction) is about three orders of magnitude higher than $\rho_{a/b}$. Furthermore, the behaviours of ρ_c and $\rho_{a/b}$ are very different; the former is semiconductor like, while the latter is metallic.

The disc-shaped single-crystal specimen had an average diameter of 2.0 mm and a thickness of 0.6 mm, in which the crystal c axis was parallel to the circular disc face. In the measurements, the direction of the applied magnetic field H_a , was perpendicular to the cylindrical symmetry axis and had an angle θ with respect to the a - b plane as shown in figure 2. The uncertainty of the angle θ was less than 0.07 rad. In this configuration, the maximum demagnetization factor was estimated to be about 0.2 when one used the anisotropic parameter $\epsilon = 0.1$ [5]. The advantage of the present arrangement was that the geometrical effect on the magnetization could in some sense be avoided (see the appendix for a discussion about demagnetization). Thus, the angle-dependent irreversible magnetic behaviour could unambiguously be obtained from the measured magnetization of the specimen.

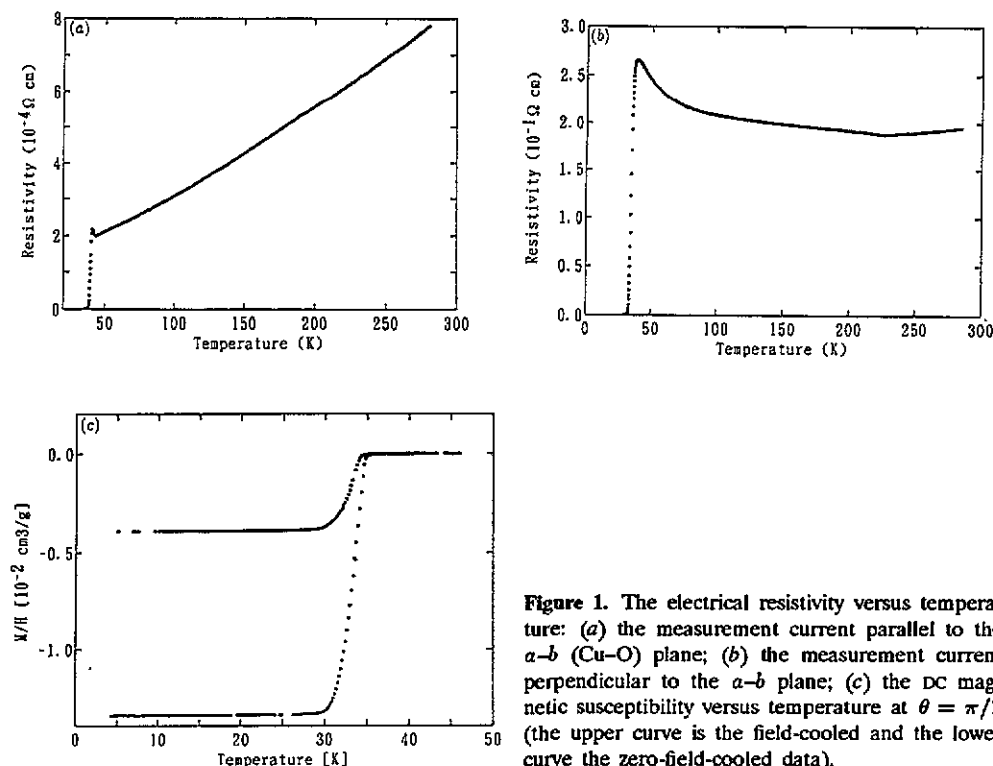


Figure 1. The electrical resistivity versus temperature: (a) the measurement current parallel to the a - b (Cu-O) plane; (b) the measurement current perpendicular to the a - b plane; (c) the DC magnetic susceptibility versus temperature at $\theta = \pi/2$ (the upper curve is the field-cooled and the lower curve the zero-field-cooled data).

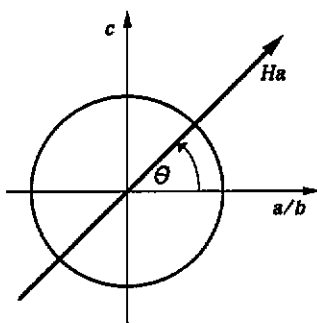


Figure 2. The side view of the configuration of the single-crystal specimen and the applied magnetic field (induction).

The magnetization was measured using a parallel-field vibrating-sample magnetometer (VSM) (EG & G Princeton Applied Research model 4500, equipped with a Janis Corporation magnet) at temperatures $T = 4.2, 10, 20$ and 30 K, under a cyclic field ± 9 T at a typical sweep rate 20 mT s^{-1} . The measurements were carried out at angles $\theta = 0, \pi/12, \pi/6, \pi/3$ and $\pi/2$.

3. Results and discussion

There are two contributions to the magnetization M : a reversible part M_{re} due to a screening current near the specimen surface and associated with the expulsion of the magnetic field, and an irreversible part M_{irr} associated with pinning of the vortices and the resultant vortex density gradient of the screening current throughout the specimen. The irreversible contribution results from pinning of the vortices as they attempt to enter or leave the specimen (in increasing or decreasing applied fields, respectively). A critical state is set up in which a vortex density gradient and a concomitant critical current J_c flows throughout the specimen, resulting in a magnetization M_{irr} [14]. The sign of the gradient, the direction of the current flow and hence the sign of M_{irr} depend on whether H_a is increasing or decreasing. J_c and hence M_{irr} depend on the magnitude of the field.

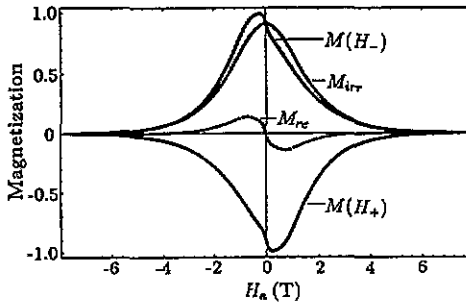


Figure 3. The magnetization versus applied field (induction) at $\theta = \pi/2$ and $T = 10$ K. $M(H_-)$ and $M(H_+)$ are the measured magnetizations corresponding to decreasing and increasing fields, respectively; M_{re} is the reversible part, and M_{irr} the irreversible part. The magnetizations were normalized by dividing by the factor $M_{max}(H_-) = 4 \times 10^5 \text{ A m}^{-1}$.

Figure 3 shows a typical magnetization curve of the specimen at $\theta = \pi/2$ and $T = 10$ K. Using the same method as in [11], the measured magnetization could be separated into two parts: the reversible component $M_{re}(H_a)$ and the irreversible component $M_{irr}(H_a)$, defined as

$$M_{re}(H_a) = \frac{1}{2}[M(H_-) + M(H_+)] \quad (1)$$

$$M_{irr}(H_a) = \frac{1}{2}[M(H_-) - M(H_+)] \quad (2)$$

where $M(H_-)$ and $M(H_+)$ are the measured magnetizations corresponding to decreasing and increasing applied magnetic fields, respectively. Concerning this separation by equations (1) and (2), it is necessary to point out that this procedure is correct only as a first approximation when the field dependence of $M_{irr}(H_a)$ is weak and it is not a good approximation to separate $M_{re}(H_a)$ when $M_{irr}(H_a)$ is much larger than $M_{re}(H_a)$. Nevertheless, this separation provides a practical way to separate the irreversible component with which we are concerned in the present study. As an example of the separation, the reversible magnetization M_{re} , and irreversible magnetization M_{irr} , are also shown in figure 3. For convenience, in the

following discussion, all magnetization data have been normalized by dividing by a (normalization) factor of $M_{\max}(T, \theta = \pi/2)$.

In the following, we shall concentrate our discussion on only the irreversible component, which is proportional to the critical current and is a real measure of the flux pinning of the superconductor. Thus, one can probe the physical picture of the flux pinning through the angle-dependent measurements of $M_{\text{irr}}(\theta)$. In particular, the experiments can be used to clarify the intrinsic pinning due to the layered structure of the materials, and the extrinsic pinning due to all other imperfections of the structure.

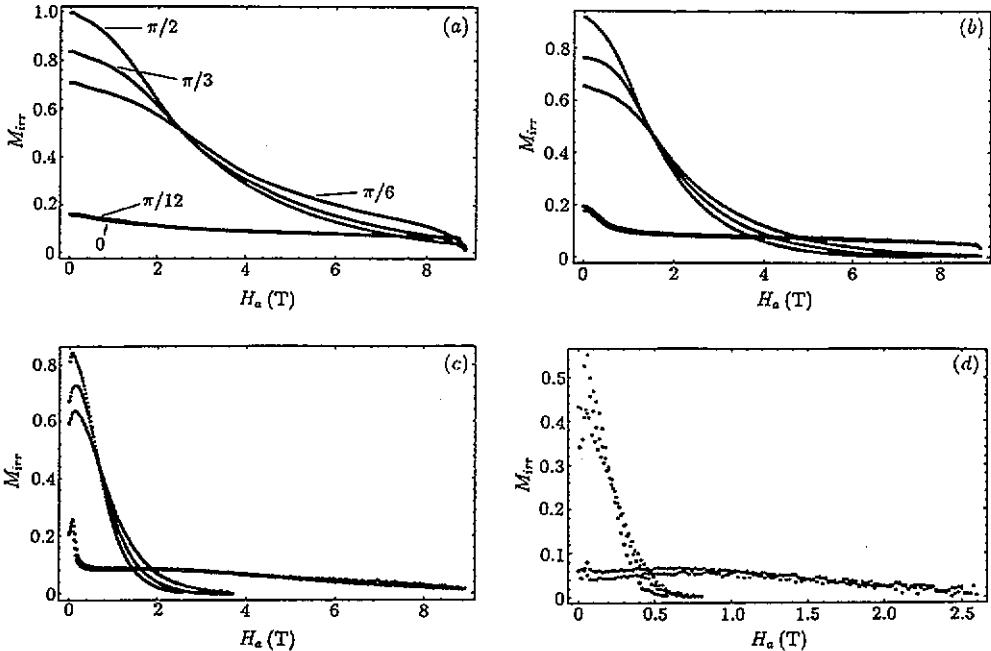


Figure 4. The (normalized) irreversible magnetic components M_{irr} versus applied magnetic field (induction) for various configuration angles: (a) $T = 4.2$ K and $M_{\max}(\pi/2) = 7.4 \times 10^5$ A m⁻¹; (b) $T = 10$ K and $M_{\max}(\pi/2) = 4.0 \times 10^5$ A m⁻¹; (c) $T = 20$ K and $M_{\max}(\pi/2) = 1.3 \times 10^5$ A m⁻¹; (d) $T = 30$ K and $M_{\max}(\pi/2) = 1.5 \times 10^4$ A m⁻¹.

Figure 4 shows the irreversible magnetization versus the applied fields for various angles at $T = 4.2, 10, 20$ and 30 K. In this wide range of temperatures, the curves of the magnetization versus applied field show qualitatively similar behaviours. The maximum values of the magnetization and the irreversible field decrease with increasing temperature, and the orders of their relative positions for the different angles are not changed.

In the experimental results of Hellman *et al* [11], the irreversible component increased less than 50% when the angle changed by $\pi/2$ for a $1 \text{ mm} \times 2 \text{ mm} \times 10 \text{ mm}$ Nb specimen. ($\pi/2$ means that the direction of the applied field, which rotated around the longest axis, changed from the short-edge direction to the long-edge direction.) This change was purely due to geometrical factors, since the upper critical field, H_{c2} , is angle independent for conventional isotropic superconductors, which was indeed shown in their experimental results. The distinguishing feature of the HTSCs

from the conventional superconductors is that there is an irreversibility line H_{irr} in the H versus T diagram, and $H_{\text{irr}}(T)$ is much smaller than the upper critical field $H_{c2}(T)$. H_{irr} could be defined as the field which corresponds to the vanish point of the irreversible magnetization, i.e. $H = H_{\text{irr}}$ when $M_{\text{irr}} = 0$ in the M versus H loop. In some sense, H_{irr} in the HTSCs plays the same role as H_{c2} in the conventional superconductors.

However, our results show that the maximum magnetization $M_{\text{max}}(\theta)$ monotonically increases (by a factor of a few) while the irreversibility line $H_{\text{irr}}(\theta)$ (obtained by extrapolating the M versus H curves for the low-temperature data), monotonically decreases (by a factor of a few), as the direction of the applied field changes from being parallel to perpendicular to the superconducting (Cu–O) plane. Furthermore, owing to the selection of the disc-shaped specimen, the geometrical effect on the M versus H_a response curve has basically been avoided in the present experiments. Therefore, the increase in $M_{\text{max}}(\theta)$ and the decrease in $H_{\text{irr}}(\theta)$ show unambiguously that the irreversible magnetic behaviour of the HTSCs is determined by the layered structure of the materials. As discussed by Kes *et al* [3], the non-superconducting (insulating) layers between the superconducting (Cu–O) layers are intrinsic pinning sites for the vortices; because of their extended spatial distribution, the paths of the supercurrents in vortices have been fundamentally modified. The extrinsic pinning sites such as impurities and dislocations are, in principle, distributed in the specimen randomly and cannot contribute to the angular dependence of the M versus H_a response curves shown in figure 4.

Recently, on the basis of the anisotropic Ginzburg–Landau (GL) theory [15], Blatter *et al* [5] introduced a scaling theory to deal with the physical properties of the HTSCs by mapping the results of isotropic superconductors onto the highly anisotropic materials. Applied to the magnetization measurements, the scaling rule may be expressed as

$$M(\theta, H_a) = \epsilon_\theta \tilde{M}(\epsilon_\theta^{-1} H_a) \quad (3)$$

where M and \tilde{M} are the anisotropic and isotropic quantities, respectively, θ the same angle as defined in this paper, and

$$\epsilon_\theta = \sqrt{\epsilon^2 \cos^2 \theta + \sin^2 \theta} \quad (4)$$

where $\epsilon^2 = m_{a/b}/m_c$; $m_{a/b}$ and m_c are the effective masses of the pair carriers in the a – b plane and along the c direction, respectively. (Blatter *et al* also rescaled the temperature with the anisotropic parameter ϵ . However, the present experiments do not support their rescaled temperature approach, so we do not write the temperature parameter in the formula.) When $\epsilon = 1$, $\epsilon_\theta = 1$ and the anisotropic system degenerates to an isotropic system. The anisotropic GL theory is based on the effective-mass model, which considers the total physical properties to be determined by the anisotropic electronic characteristics of the materials. Thus, ϵ_θ is the factor that scales an electromagnetic quantity from an anisotropic representation into an isotropic description. Somehow, owing to the high anisotropy of HTSCs ($\epsilon \ll 1$), from equation (4) it is easy to see that ϵ_θ is mainly controlled by the sine term, i.e. $\epsilon_\theta \approx \sin \theta$ except for the very small angles. Therefore, in the present experiment, it is difficult to obtain the value of ϵ without very precise angle measurements. On the other hand, in this extreme condition $\epsilon \ll 1$, it is only the c -direction component of

the magnetic field that can effectively contribute to the change in a physical parameter. The Bi-based and Tl-based HTSCs are these kinds of material as discussed by Kes *et al* [3].

According to the scaling theory of Blatter *et al*, if we replot the $M(\theta)$ versus $H_a(\theta)$ curves using the scaling parameters $M(\theta)/\epsilon_\theta$ and $H_a(\theta)\epsilon_\theta$, the angle-dependent M versus H_a curves should be rescaled onto one unique (angle-independent) curve when the temperature is not taken into account. Kes *et al* [3] classified two kinds of flux pinning in the HTSC materials: the intrinsic pinning, i.e. a pinning effect by the multilayer structure itself, and the extrinsic pinning due to the preparation, i.e. voids, precipitates, crystallographic defects, etc. In this sense, the scaling approach of Blatter *et al* should be valid for the intrinsic pinning, but not for the extrinsic pinning.

We have tried to use equation (3) to scale our data. Qualitatively, our experimental results are in agreement with the scaling theory, but the experimental data show clear deviations from the quantitative predictions of the theory of Blatter *et al*. Nevertheless, our angle-dependent data clearly show different features for small and large angles, respectively. For small angles, the curves are almost identical for the values of $\theta = 0$ and $\pi/12$ at which we performed the measurements. However, prompted by the theory of Blatter *et al* [5], we have found temperature-independent empirical scaling factors $f(\theta)$ to scale the large-angle ($\pi/6$, $\pi/3$ and $\pi/2$) data and have achieved excellent scaling results at relatively high fields. Three points should be made:

(1) The values of $f(\theta)$ were obtained by rescaling the data obtained at 10 K. Somehow, it turns out that the same $f(\theta)$ could rescale the data obtained at 4.2, 20 and 30 K fairly well although the 4.2 K data show a very small deviation.

(2) At the present time, limited by the experimental data, we cannot obtain an analytic expression of the empirical scaling factor $f(\theta)$ but only a set of numerical data.

(3) When we tried to rescale the large-angle data, we did not consider the high-field portion of the $M-H$ loop where the field sweep direction is reversed. The high-field-portion data are the curved parts in figure 5(a), which are artifacts of the measurements and of course deviate from scaling. These artifacts can be eliminated if one can apply a higher field (up to or over H_{irr}). Since H_{irr} is a decreasing function of temperature, the deviations from scaling at high values of $H_a(\theta)f(\theta)$ appear only in the low-temperature (here 4.2 K) curves, but do not appear in the high-temperature (here 10, 20 and 30 K) data. For the latter, $H_{irr} < 6$ T which is the limit of our VSM machine.

As shown in figure 5, the angle-dependent $M(\theta)$ versus $H_a(\theta)$ curves have been quite reasonably rescaled into the unique angle-independent $M(\theta)/f(\theta)$ versus $H_a(\theta)f(\theta)$ curve for the large-angle data, however, the small-angle data cannot be rescaled in this way. For comparison, we plot ϵ_θ (with $\epsilon = 0.1$) and $f(\theta)$ in figure 6. One can clearly see the deviation of $f(\theta)$ from ϵ_θ even after considering the angle uncertainty and the changes in the demagnetization factors with angle.

The scaling characteristics of the angle-dependent M versus H_a curves shown in figure 5 reflect the fact that the intrinsic pinning sites of the insulating layers dominate the electromagnetic properties for the high-quality HTSC single crystals before some artificial defects are created by radiation and plantation, etc. The *insulating* layers are regularly oriented parallel to the superconducting (Cu-O) planes and change the

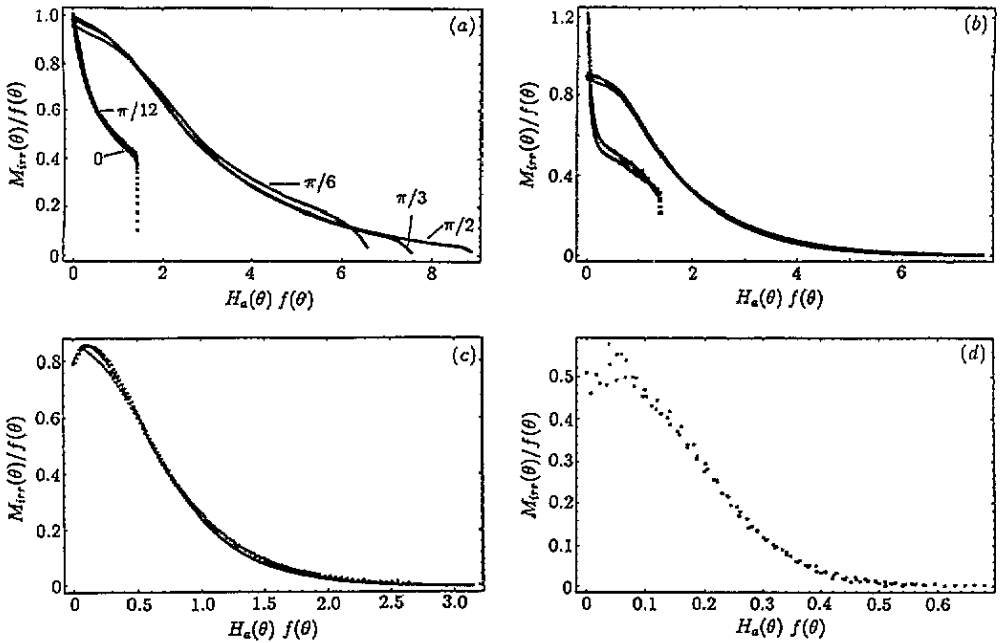


Figure 5. The rescaled results shown in figure 4: (a) $T = 4.2$ K and $M_{\max}(\pi/2) = 7.4 \times 10^5$ A m⁻¹; (b) $T = 10$ K and $M_{\max}(\pi/2) = 4.0 \times 10^5$ A m⁻¹; (c) $T = 20$ K and $M_{\max}(\pi/2) = 1.3 \times 10^5$ A m⁻¹; (d) $T = 30$ K and $M_{\max}(\pi/2) = 1.5 \times 10^4$ A m⁻¹. In (c) and (d), the small-angle data were not plotted.

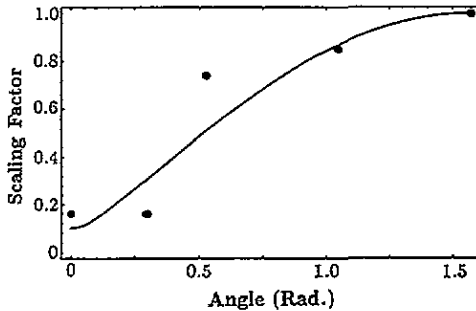


Figure 6. The empirical (normalized) scaling factors $f(\theta)$. The values of $f(0)$ and $f(\pi/12)$ were obtained through $M_{\max}(0)/M_{\max}(\pi/2)$ and $M_{\max}(\pi/12)/M_{\max}(\pi/2)$, which could not rescale the M versus H curves but were for comparison with ϵ_θ . As a comparison, the full curve shows the scaling factors $\epsilon_\theta = \sqrt{\epsilon^2 \cos^2 \theta + \sin^2 \theta}$ given in [5] with $\epsilon = 0.1$.

paths of the supercurrents. The confinement of the supercurrents is much stronger than the localization of the vortices by the crystallographic defects and reflects the physical properties of the intrinsic pinning which can be probed by the magnetization measurements. Thus, the investigation of the angle-dependent M versus H_a curves through the scaling approach in the present results manifests itself in the intrinsic behaviour of the La-based HTSC single crystals.

It may be interesting to compare the present results with the magnetization

measurements recently performed by Fischer *et al* [12] on a Y1:2:3 single crystal at $T = 77$ K. Using the scaling parameters $M/\sin\theta$ and $H_a \sin\theta$, Fischer *et al* scaled the M versus H_a curves onto a unique curve fairly well for $\theta \geq \pi/6$. For $\theta \leq \pi/6$, the data could not be rescaled by the simple scaling factor $\sin\theta$. (Note that in their paper the definition of the angle α is different from this paper.)

From the results of Fischer *et al* [12] on Y1:2:3 and figures 4 and 5 of the present paper, one may conclude that there seems to be a critical angle θ_c : for $\theta > \theta_c$, the irreversible magnetization, M_{irr} , can be fairly well rescaled but, for $\theta < \theta_c$, the scaling approach may not hold. To check this argument will require a large-angle-resolution apparatus. At the present time we cannot perform high-accuracy angle-dependent measurements because of instrumental limitations.

It is worthwhile to emphasize that the empirical scaling factor $f(\theta)$ is almost temperature independent in the range over which we performed the measurements (4.2–30 K; the corresponding reduced temperature $t = T/T_c$ is in the range 0.12–0.86). In the future, it would be valuable to carry out experiments with high-accuracy instruments over a more extended range of temperatures to probe the temperature dependence of the scaling factor $f(\theta)$.

The temperature-independent scaling behaviour has very important physical implications. For example, it can be applied to the determination of the irreversible magnetic field values at low temperatures. To our knowledge, so far there is no effective way of directly measuring the irreversible fields of the HTSCs at relatively low temperatures. Nevertheless, our temperature-independent scaling approach provides a practical experimental method of finding $H_{irr}(\theta)$. One can first find the scaling factors $f(\theta)$, at a relatively high temperature, second obtain the smallest value of $H_{irr}(\theta)$ ($\theta = \pi/2$) at low temperatures and finally employ $f(\theta)$ unambiguously to determine the angle-dependent irreversible field $H_{irr}(\theta)$.

One point which should be made is that the present scaling approach is based on the anisotropic structure of the materials (the layers between two superconducting layers considered as intrinsic pinnings) and seems to be not valid for the irreversible properties due to extrinsic pinning sites such as point defects, dislocations and vacancies. Therefore, the same scaling factor may not be used for changes in irreversible properties due to some artificial techniques, such as irradiation and ion implantation.

Another feature of the experimental results concerns the scaling property as a function of temperature at a fixed angle. As we know, the critical current density, J_c , is basically determined by the irreversible magnetization M_{irr} [14], i.e. $J_c \propto M_{irr}$, and as a consequence, the flux pinning force $f_{pinning}$ is proportional to the product of the irreversible magnetization and the applied field, i.e. $f_{pinning} = CM_{irr}H_a$, where C is a constant determined by the geometrical factor and the electromagnetic units used. In order to check the properties of the pinning forces, we have studied the reduced pinning forces $f_{pinning}/f_{p,peak}$, as a function of the reduced field $b = H_a/H_{irr}$. The experiments show that, in a wide range of temperatures (4.2–20 K; the corresponding reduced temperatures, t , are 0.12–0.57), the curves of $f_{pinning}/f_{p,peak}$ versus H_a/H_{irr} can be rescaled into one unique curve. This indicates that the volume pinning force obeys the Fietz–Webb scaling law [16]. Figure 7 shows typical results obtained at $\theta = \pi/2$. A scaling law of the form

$$f_{pinning}(B) = CM_{irr}H_a = f_0H_{irr}^n b^p (1-b)^q \tag{5}$$

appears to be valid for these results, with approximate values $p = 1$ and $q = 4$,

whereas n was found to be equal to 2 from the log-log plot of the maximum pinning forces $f_{p,peak}$, against irreversible fields H_{irr} , as shown in figure 8. This is in agreement with a previous result [17]. The experimental results for $\theta = \pi/3$ and $\pi/6$ show similar behaviours.

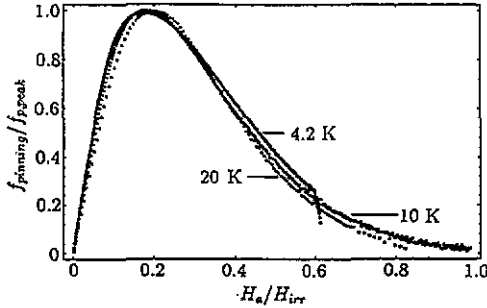


Figure 7. The (normalized) pinning force $f_{pinning}/f_{p,peak}$, versus (reduced) magnetic field H_a/H_{irr} , at various temperatures $T = 4.2, 10$ and 20 K at $\theta = \pi/2$.

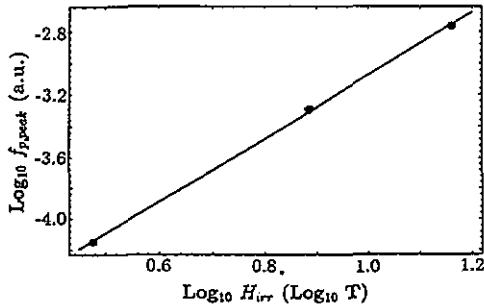


Figure 8. The log-log plot of the maximum pinning force $f_{p,peak}$, versus irreversible field H_{irr} , from the data shown in figure 7 (au, arbitrary units). A least-squares fit to a straight line gives a slope $n = 2.0$.

The physical basis of the scaling approach is the effective-mass model, in which only the anisotropic characteristics of the electromagnetic properties of the materials have been taken into account. The details of the coupling between the superconducting (Cu-O) layers have not been considered. This is really a very basic question to answer. However, at present, there is no critical experiment to clarify the nature of the inter-layer coupling. On the one hand, both the effective-mass model and the Lawrence-Doniach (LD) [18] model have been used to interpret the experimental results and to some extent to provide a reasonable explanation. On the other hand, these two models are based on different physical pictures. The Josephson junction is the basic mechanism of the LD model, but the effective-mass model does not consider the existence of this quantum phenomenon. From the correspondence principles of physics, the microscopic behaviour of a system must obey quantum mechanics; however, when the number of *particles* in the system is large enough,

the microscopic kinetic equations should be approximated by the classical equations with $\hbar \rightarrow 0$ (\hbar is Planck's constant). To our knowledge, there has not yet been any theoretical treatment of the correspondence between the LD model and effective-mass model. It is not even clear whether such a correspondence should exist.

4. Summary

Using a VSM we have investigated the angle-dependent magnetization of a high-quality disc-shaped $\text{La}_{1.87}\text{Sr}_{0.13}\text{CuO}_4$ single crystal over the temperature range 4.2–30 K (the corresponding reduced temperatures are in the range 0.12–0.86). After separating the irreversible component from the measured magnetization induced by the applied field, we have confirmed that the irreversible magnetization of the highly anisotropic HTSCs behaves very differently from that of conventional isotropic superconductors as a function of the angle between the direction of the applied field and the superconducting plane. The angular dependence of the irreversible magnetization may be classified into two distinct regions: the small-angle data seem to be identical and the large-angle data could be rescaled into a unique curve by an empirical factor. The empirical scaling factor is qualitatively consistent with a scaling theory recently introduced by Blatter *et al.* The scaling properties of the pinning forces have been discussed in terms of the Fietz–Webb scaling law for a wide range of temperatures.

Acknowledgments

The present work was in part supported by a Grant-in-Aid for Scientific Research from the Ministry of Education, Science and Culture of Japan. One of the authors (ZJY) would like to thank Professor K Kitazawa for hospitality during his stay in Tokyo and helpful discussion, and to acknowledge Dr R A Dunlap for proof reading the manuscript.

Appendix

For an isotropic material, the demagnetization factor is a constant along any radial direction for a perfect round disc sample. However, for an anisotropic material, the unique demagnetizing field can be defined only for ellipsoidal shapes. With the lowest order of approximation, one may estimate the demagnetization factor easily:

$$N_c = x \quad N_{a/b} = x/\epsilon \quad N_{\text{axis}} = (x/\epsilon)(2/0.6) \quad (\text{A1})$$

correspond to the demagnetization factors along the c direction, in the a/b plane, and along the rotation axis of the disc. Using the equality

$$N_{a/b} + N_c + N_{\text{axis}} = 1 \quad (\text{A2})$$

one can solve the equation easily. One may choose a commonly accepted value $\epsilon = 0.1$, and then one obtains

$$N_c \approx 0.022 \quad N_{a/b} \approx 0.22 \quad N_{\text{axis}} \approx 0.75. \quad (\text{A3})$$

References

- [1] Kogan V G 1988 *Phys. Rev. B* **38** 7049
- [2] Naughton M J, Yu R C, Davies P K, Fischer J E, Chamberlin R V, Wang Z Z, Jing T W, Ong N P and Chaikin P M 1988 *Phys. Rev. B* **38** 9280
- [3] Kes P H, Aarts J, Vinokur V M and van der Beek C J 1990 *Phys. Rev. Lett.* **64** 1063
- [4] Hao Z D and Clem J R 1991 *Phys. Rev. B* **43** 7266
- [5] Blatter G, Geshkenbein V B and Larkin A I 1992 *Phys. Rev. Lett.* **68** 875
Hao Z D and Clem J R 1992 *Phys. Rev. B* **46** 5853
- [6] Yuan S L *et al* 1992 to be published
- [7] Farrell D E, Bonham S, Foster J, Chang Y C, Jiang P Z, Vandervoort K G, Lam D J and Kogan V G 1989 *Phys. Rev. Lett.* **63** 782
Okuda K and Kawamata S 1992 *Japan. J. Appl. Phys.* **7** 279
- [8] Martin S, Fiory A T, Fleming R M, Schneemeyer L F and Waszczak J V 1988 *Phys. Rev. Lett.* **60** 2194
- [9] Iye J, Watanabe A, Nakamura S, Tamagai T, Terashima T, Yamamoto K and Bando Y 1989 *Physica C* **167** 278
- [10] Kitazawa K, Kambe S, Naito M, Tanaka I and Kojima H 1989 *Japan. J. Appl. Phys.* **28** L555
- [11] Hellman F, Gyorgy E G and Dynes R C 1992 *Phys. Rev. Lett.* **68** 867
- [12] Fischer P, Busch R, Neumüller H W, Ries G and Braun H F 1992 *Supercond. Sci. Technol.* **5** S440
- [13] Kimura T, Kishio K, Kobayashi T, Nakayama Y, Motohira N, Kitazawa K and Yamafuji K 1992 *Physica C* **192** 247
- [14] Bean C P 1964 *Rev. Mod. Phys.* **36** 31
Däumling M and Larbalestier D C 1989 *Phys. Rev. B* **40** 9350
- [15] Tinkham M 1964 *Phys. Lett.* **9** 217
- [16] Campbell A M and Evetts J E 1972 *Critical Currents in Superconductors* (London: Taylor & Francis) p 159
- [17] Kishio K, Nakayama Y, Motohira N, Noto T, Kobayashi T, Kitazawa K, Yamafuji K, Tanaka I and Kojima H 1992 *Supercond. Sci. Technol.* **5** S69
- [18] Lawrence W E and Doniach S 1971 *Proc. 12th Int. Conf. on Low Temperature Physics (Kyoto, 1970)* ed E Kanda (Tokyo: Keigaku) p 361